ACS Catalysis

Letter

pubs.acs.org/acscatalysis

Death and Rebirth: Photocatalytic Hydrogen Production by a Self-Organizing Copper–Iron System

Steffen Fischer,[†,‡] Dirk Hollmann,[‡] Stefanie Tschierlei,[§] Michael Karnahl,[‡] Nils Rockstroh,[‡] Enrico Barsch,[†,‡] Patrick Schwarzbach,[§] Shu-Ping Luo,[‡,∥] Henrik Junge,[‡] Matthias Beller,[‡] Stefan Lochbrunner,[§] Ralf Ludwig,[†,‡,*] and Angelika Brückner*[,‡]

[†]Institute of Chemistry, Department Physical Chemistry, University of Rostock, Dr. Lorenz-Weg 1, 18059 Rostock, Germany

[‡]Leibniz Institute for Catalysis at the University of Rostock, Albert Einstein-Straße 29a, 18059 Rostock, Germany

[§]Institute of Physics, University of Rostock, Universitätsplatz 3, 18055 Rostock, Germany

[∥]State Key Laboratory Breeding Base of Green Chemistry-Synthesis Technology, Zhejiang University of Technology, 310014 Hangzhou, China

Supporting Information

ABSTRACT: This study provides detailed mechanistic insights into light-driven hydrogen production using an abundant copper–iron system. It focuses on the role of the heteroleptic copper photosensitizer $[Cu(P\text{^}P)(N\text{^}N)]^+$, which can be oxidized or reduced after photoexcitation. By means of IR, EPR, and UV/vis spectroscopy as well as computational studies and spectroelectrochemistry, the possibility of both mechanisms was confirmed. UV/vis spectroscopy revealed the reorganization of the original heteroleptic photosensitizer during catalysis toward a homoleptic $[Cu(N\text{^}N)_2]^+$ species. Operando FTIR spectroscopy showed the formation of a catalytic diiron intermediate, which resembles well-known hydrogenase active site models.

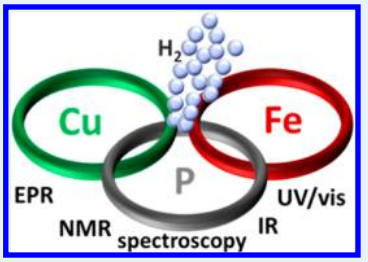

KEYWORDS: *proton reduction, iron catalysts, copper photosensitizer, operando spectroscopy, catalytic intermediates*

The global rising population and energy demand are leading to a faster depletion of fossil resources and boost the search for sustainable alternatives.[1,2] These options ideally utilize natural energy sources such as water, wind or solar power that produce no waste and emissions such as carbon dioxide.[3,4] A second major requirement is the constant availability of energy, which calls for efficient energy storage materials and capacities.[5] Currently, several approaches are controversially discussed in the literature, ranging from electricity storage in batteries and supercapacitors to chemical energy storage mainly in hydrogen or hydrogen-releasing molecules (liquid organic hydrogen carriers).[6] In particular, hydrogen is very attractive because of its high energy content and clean combustion.[7] However, sustainable hydrogen production from water using sunlight is still demanding and needs further improvement in several aspects, such as the replacement of noble metals, increased efficiency, use of pure visible light and a thorough understanding of the underlying processes.[8,9] Recent progress on the replacement of noble metals showing high hydrogen production rates for a system composed of a nonprecious iron water reduction catalyst (WRC), a heteroleptic copper photosensitizer (CuPS **1**), and triethylamine acting as sacrificial reductant (SR) was made in our groups.[10−12]

Systematic variation of the CuPS and its ligand structure resulted in the most efficient fully noble-metal-free hydrogen generating system so far, with a maximum turnover number (TON_H) of 1330.[12,15] However, the lifetime of the overall catalytic system varied from 5 to 60 h, depending on the applied conditions and copper complexes. Preliminary experiments suggested the predominance of an oxidative reaction pathway in which the CuPS is first oxidized after photoexcitation (Scheme 1).

Interestingly, negligible activity was observed with the homoleptic sensitizer $[Cu(N\text{^}N)_2]^{2+}$ (CuPS **2**) with two phenanthroline ligands, although it also absorbs UV–vis light and should thus be able to act as a photosensitizer, as well. The missing activity may be due to two possible reasons: The redox potentials required for the electron transfer are not sufficient[13] or the lifetime of the excited triplet state of complex **2** is too short.[14]

Information about the different activation and deactivation pathways of the iron WRC and the CuPS as well as their catalytic intermediates is still rare. Thus, a detailed understanding of the catalytic cycle may contribute to the development of more efficient systems. Therefore, it was the aim of this study to investigate the mechanism of the light-driven production of hydrogen by a heteroleptic CuPS and an iron WRC using several methods, such as operando FTIR spectroscopy, UV/vis and in situ EPR spectroscopy, as well as their combinations with spectroelectrochemical[16,17] techniques.

Received: March 24, 2014
Revised: April 29, 2014

   dx.doi.org/10.1021/cs500387e | *ACS Catal.* 2014, 4, 1845−1849

Scheme 1. Reductive (red) and Oxidative (blue) Reaction Pathway and the Initial Structures of the Applied Copper Photosensitizer (CuPS, e.g., 1) and Water Reduction Catalyst (WRC)

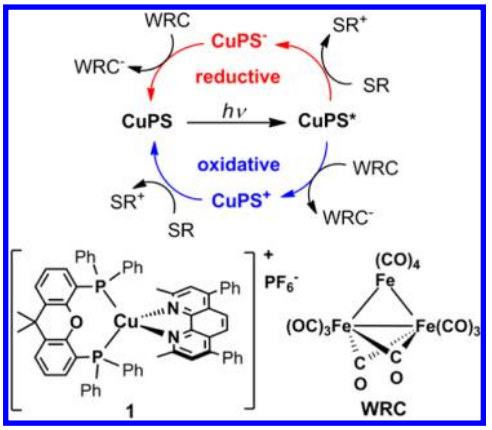

The experimental results are supported by computational studies as well as by catalytic measurements.

The heteroleptic copper complex **1** $[Cu(P^{\wedge}P)(N^{\wedge}N)]^+$, which contains bidentate P^P (Xantphos) and N^N (2,9-dimethyl-4,7-diphenyl-1,10-phenanthroline) chelate ligands, exhibits a distorted tetrahedral structure of the Cu^+ center in the ground state (Scheme 1).[18−20] Upon photoexcitation, a metal-to-ligand charge transfer (MLCT) to the phenanthroline ligand occurs, followed by a structural transformation to a triplet excited state; with a more square planar geometry in terms of the ligand orientation around the formal Cu^{2+} center; and finally, an intersystem crossing.[21] This long-lived excited state can now be reduced or oxidized, depending on the reaction partners in the catalytic system, resulting in $\mathbf{1}^-$ or $\mathbf{1}^+$, respectively.[14] Both pathways could be considered to be responsible for photocatalytic activity. At the beginning, the reductive pathway was investigated by means of EPR spectroscopy. In this context, a reduced CuPS was detected under UV/vis irradiation in the presence of triethylamine (TEA), which acts as a sacrificial reductant (Figure 1a).

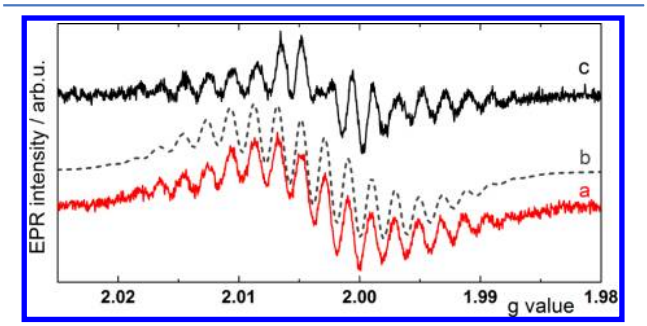

Figure 1. EPR spectra of (a) CuPS **1** in THF/TEA (4/1) under UV/vis irradiation, (b) the respective EPR simulation (g = 2.0034, line width ΔB = 2.5G, $2 \times A_H$ = 10.0G, $2 \times A_H$ = 7.0G, $2 \times A_N$ = 3.4G, $1 \times A_{Cu}$ = 3.4G), and (c) $\mathbf{1}^-$ obtained at −1.5 V vs Ag/Ag^+.

Analysis of the superhyperfine structure (shfs) revealed the coupling of the free electron to all hydrogen and nitrogen nuclei of the aromatic system in the phenanthroline ligand ($4 \times H$ (I = 1/2), $2 \times N$ (I = 1)) as well as to the copper nucleus (I = 3/2) (Figure 1b). In combination with the g value of 2.0034, which is close to that of the free electron, the shfs coupling constants suggest a complete electron delocalization within the N^N ligand,[22] in contrast to a partial ligand-metal delocalization observed in an analogous iridium photosensitizer (IrPS).[23] This finding was further supported by EPR spectroelectrochemistry, providing the same EPR spectrum (Figure 1c). Moreover, the full reversibility of the reductive cycle along with the high stability of complex **1** under reductive conditions was proven by UV/vis absorption spectroscopy (Supporting Information (SI) Figures S1, S2). Here, the electrochemical as well as the photochemical reduction did not lead to any changes in the absorption behavior.

In contrast to the reductive pathway, the formation of $\mathbf{1}^+$ within an oxidative pathway can occur with $[Fe_3(CO)_{12}]$ as an electron acceptor (Scheme 1). Applying EPR spectroscopy, characteristic decomposition products $[Fe_3(CO)_{12}]^{\bullet-}$, $[Fe_3(CO)_{11}]^{\bullet-}$, and $[Fe_2(CO)_8]^{\bullet-}$, which were detected for the analogous IrPS system, as well,[24] were monitored. Neither $Cu^{II}PS$[25] nor $Cu^{I}PS^+$ species have been detected in the present study. Even with EPR spectroelectrochemistry (+1.5 V vs Ag/Ag^+), no oxidized copper complex was observed, indicating an unexpected reaction pathway under oxidative conditions.

This oxidation pathway was examined by UV/vis spectroscopy, which can distinguish among various redox states of the copper species by their different MLCT transitions. For instance, in complex **1** only the phenanthroline moiety contributes to the MLCT transition around 390 nm. This band decreases after several redox cycles, each composed of an oxidation step, followed by a rereduction process (Figure 2),

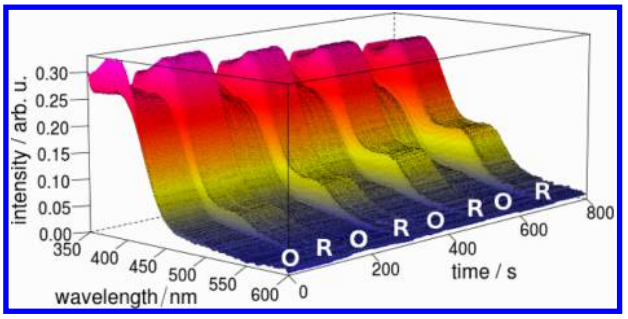

Figure 2. Oxidation (O, +1.5 V) and rereduction (R, at −0.5 V vs Ag/Ag^+) cycles (duration of each step: 100 s) of **1** in acetonitrile solution monitored by UV/vis spectroelectrochemistry.

indicating that the concentration of **1** in the solution becomes lower. Furthermore, a new band at 475 nm rises during each rereduction step, which corresponds to the well-known homoleptic CuPS $[Cu(N^{\wedge}N)_2]^+$ (**2**), showing an absorption band exactly in this range (see SI). Thus, the concentration of the new generated complex **2** increases during the redox cycles. Consequently, the concentration of the oxidized species $\mathbf{2}^+$, formed within these oxidation steps, also rises. However, the absorption spectra of the oxidized species $\mathbf{1}^+$ (still present) and $\mathbf{2}^+$ (gradually formed) during the several oxidation processes are almost identical, which is caused by the exclusive contribution of the phenanthroline ligand to the MLCT transition in the respective complexes (O in Figure 2).

In addition, the absorption spectra were measured under photochemically induced oxidative conditions with methylviologen (MV, 1,1′-dimethyl-4,4′-bipyridinium dichloride) as chemical oxidant and light irradiation at 350 nm.[26,27] Again, the MCLT band of **1** decreases, and the band of complex **2** appears in the visible region over time (SI Figure S2).

dx.doi.org/10.1021/cs500387e | ACS Catal. 2014, 4, 1845−1849

As mentioned above, the absorption behavior suggests that the original heteroleptic complex **1** is decomposed exclusively under the oxidative conditions by a dissociation of the sterically demanding diphosphine ligand. Indeed, DFT calculations of the oxidized species of **1** point to an elongation of the Cu−P bond from 0.233 nm (**1**) to 0.239 nm ($\mathbf{1}^{+}$) and 0.240 nm in ($\mathbf{1}^{2+}$) and to a decreasing P−Cu−P bite angle in the order 116.8° (**1**) > 109.2 ($\mathbf{1}^{+}$) > 103.2 ($\mathbf{1}^{2+}$), which provides further evidence for the proposed dissociation reaction (SI Table S1). However, this dissociation does not lead to a complete destruction of the structure of **1**. Instead, a second phenanthroline ligand coordinates to resaturate the copper center, forming the homoleptic complex $[Cu(N^{\wedge}N)_2]^{+}$ **2**. This dynamic ligand exchange between hetero- and homoleptic copper complexes was also recently reported for related CuPS.[18]

Following the aforementioned results, the crucial role of the diphosphine ligand became obvious. Caused by an electrochemical oxidation of **1**, without $[Fe_3(CO)_{12}]$ as electron acceptor, the P^P ligand is converted to Xantphosdioxide, as proven by ^{31}P NMR spectroscopy (SI Figure S4).[28] In contrast, the irradiation of **1** in the presence of the electron acceptor MV does not lead to Xantphosdioxide, revealing a different mechanism under photooxidative conditions (SI Figure S4). Thus, especially the role of the electron acceptor seems to determine the respective reaction.

Consequently, the reaction of the diphosphine ligand with the iron precursor $[Fe_3(CO)_{12}]$ has been studied by operando FTIR spectroscopy. Starting with **1** and $[Fe_3(CO)_{12}]$ in a solution of THF/TEA/H_2O, the conversion of the iron precursor to $[HFe_3(CO)_{11}]^{-}$ is observed within the first minute of irradiation, giving rise to characteristic bands at 2064(w), 1999(s), 1993(s), 1975(m), and 1748(m) cm^{-1} (Figure 3, red).[24,29] This complex is already known as active WRC in related iridium-based photocatalytic systems.[24,29] As the reaction proceeds, $[HFe_3(CO)_{11}]^{-}$ is transformed into $[Fe_2(\mu\text{-}PPh_2)(\mu\text{-}CO)(CO)_6]^{-}$ (**3**) with four intense bands at 2015(m), 1965(vs), 1934(m), 1916(s) cm^{-1} (Figure 3, blue). This transformation is accompanied by an enhanced hydrogen evolution (Figure 3, black curve). Temporarily appearing intermediate complexes are not identified yet (SI Figure S5). After 35 h, **3** is the only carbonyl compound present in solution. In the further course, its concentration drops after 120 h, which is consistent with the end of hydrogen evolution, showing the catalytic relevance of this species (SI Figure S6).

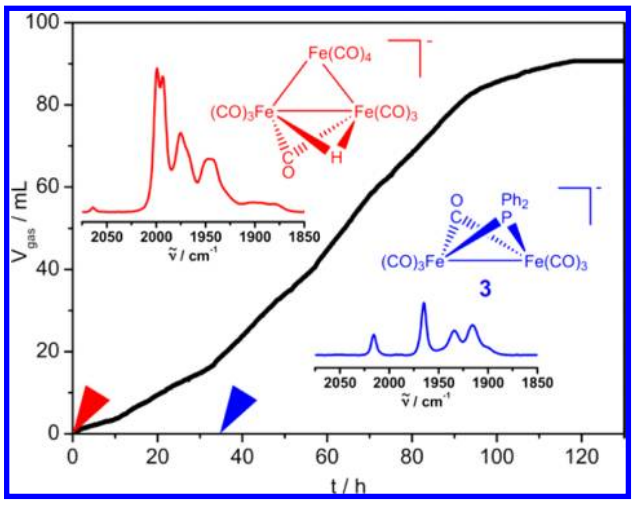

Figure 3. Results of the operando FTIR measurements: gas evolution curve (black) and IR spectrum of the solution at t = 1 min (red) and t = 35 h (blue). Conditions: 7.0 μmol of **1**, 10.0 μmol of $[Fe_3(CO)_{12}]$, 20 mL of THF/TEA/H_2O (4/1/1), visible light irradiation (1.5 W), 25 °C.

The assignment of **3** is supported by spectral data specified in works of Ellis, Walther, or Best et al.[30−32] (SI Table S2) and by DFT calculations (SI Figure S7). Its structure is analogous to monoreduced diiron hydrogenase mimics, which possess similar IR patterns.[33−36] The present PPh_2 ligand most probably originates from the decomposition of free Xantphos,[37] which is closely related to observations made with PPh_3 in the presence of hydrogen or heat.[38,39]

After complete conversion of $[Fe_3(CO)_{12}]$ to **3**, assured by operando FTIR spectroscopy, a sample of the reaction mixture was analyzed by means of NMR spectroscopy. The respective ^{31}P NMR spectrum (Figure 4, blue) displays a singlet peak at δ = 126.9 ppm, which is in good agreement with the chemical shift of **3**.[31,32]

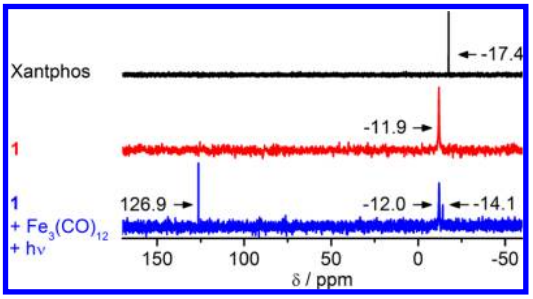

Figure 4. ^{31}P NMR investigations: black, free Xantphos ligand; red, **1**; blue, 21.3 μmol of **1** and 22.6 μmol of $[Fe_3(CO)_{12}]$ in 20 mL of solvent mixture after 5.5 h of visible light irradiation (6 W). All compounds were dissolved in THF/TEA/H_2O (4/1/1).

The additional signal at δ = −12.0 ppm can be assigned to complex **1**, showing that even after long reaction times, some **1** is still left, whereas the small signal at δ = −14.1 ppm does not match to the uncoordinated Xantphos and remains unassigned. The corresponding ^{1}H NMR spectrum of the reaction mixture reveals no hydride signal, which supports the structural assignment of the catalytically active species **3**.

Indeed, application of the homoleptic complex **2** along with the Xantphos ligand and $[Fe_3(CO)_{12}]$ yielded the same photocatalytic activity as determined for **1** and $[Fe_3(CO)_{12}]$ (Figure 5 and SI Table S4). The respective turnover numbers ($TON_{H,Cu}$) and frequencies (TOF) are nearly the same within the error of the catalytic experiments (SI Table S4). Note that under these conditions, CuPS **1** has been detected by ^{31}P NMR. This indicates a ligand exchange that leads to a "rebirth" of the active photosensitizer **1**.

It can be concluded that in both cases, the catalytic activity originates from the same dinuclear iron-diphenylphosphido species **3**, arising from a self-organization process. The nature of this essential species was further proven by an experiment without the diphosphine ligand, in which no activity could be observed (Figure 5, gray curve). Hence, the diphenylphosphido fragment is a crucial part of the active species, and only its existence enables an efficient hydrogen production within this fully noble-metal-free system.

In the present work, the mechanism and catalytic intermediates of the photoinduced iron-catalyzed hydrogen

dx.doi.org/10.1021/cs500387e | ACS Catal. 2014, 4, 1845−1849

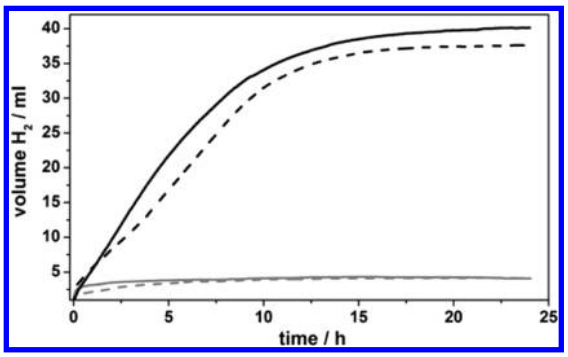

Figure 5. Hydrogen evolution curves using CuPS (5 μmol) in the presence of $[Fe_3(CO)_{12}]$ (5 μmol) as WRC in a mixture of THF/TEA/H_2O (4/3/1, 10 mL). Black dashed, **1**; black solid, **2** with Xantphos (5 μmol); gray solid, **2** without Xantphos; gray dashed, only Xantphos and $[Fe_3(CO)_{12}]$. See SI Table S4.

production in the presence of a heteroleptic CuPS were investigated. First, the attention was focused on the photosensitizer, which could be oxidized or reduced after photoexcitation. UV/vis and in situ EPR spectroscopy and their combination with electrochemistry revealed the existence of both an oxidative and a reductive pathway. The latter one is reversible with respect to the CuPS. Instead, the obtained results for the oxidative pathway, supported by DFT calculations, evidenced a photoinduced reassembling of the copper-bound ligands forming partly a homoleptic phenanthroline complex. After liberation from copper, the uncoordinated phosphine ligand releases a (PPh_2) fragment, which reacts with $[Fe_3(CO)_{12}]$ to $[Fe_2(\mu\text{-}PPh_2)(\mu\text{-}CO)(CO)_6]^-$ (**3**). The structural assignment of this catalytic intermediate was confirmed by operando FTIR and NMR spectroscopy as well as DFT.

This unique self-organizing process provides a comfortable access to an efficient and fully noble-metal-free system for the photocatalytic reduction of protons without demanding synthesis. Furthermore, the detailed understanding of the mechanism supports rational catalyst design.

■ ASSOCIATED CONTENT

Ⓢ Supporting Information

Experimental and catalytic details, UV/vis spectroelectrochemical data, IR spectra, and DFT calculations. This material is available free of charge via the Internet at http://pubs.acs.org.

■ AUTHOR INFORMATION

Corresponding Authors

*Fax: (+49) 381 498 6524. E-mail: ralf.ludwig@uni-rostock.de.
*Fax: (+49) 381 1281 51244. E-mail: angelika.brueckner@catalysis.de.

Notes

The authors declare no competing financial interest.

■ ACKNOWLEDGMENTS

Financial support from the Federal Ministry of Education and Research of Germany (BMBF) within the project "Light2-Hydrogen" is gratefully acknowledged.

■ REFERENCES

(1) Lewis, N. S.; Nocera, D. G. *Proc. Natl. Acad. Sci. U.S.A.* **2006**, *103*, 15729−15735.
(2) Armaroli, N.; Balzani, V. *Angew. Chem., Int. Ed.* **2007**, *46*, 52−66.
(3) Schiermeier, Q.; Tollefson, J.; Scully, T.; Witze, A.; Morton, O. *Nature* **2008**, *454*, 816−823.
(4) Armaroli, N.; Balzani, V. *Energy for a Sustainable World − From the Oil Age to a Sun-Powered Future*; Wiley-VCH: Weinheim, 2010.
(5) Jacobson, M. Z. *Energy Environ. Sci.* **2009**, *2*, 148−173.
(6) Styring, S. *Faraday Discuss.* **2012**, *155*, 357−376.
(7) Amouyal, E. *Sol. Energy Mater. Sol. Cells* **1995**, *38*, 249−276.
(8) Du, P.; Eisenberg, R. *Energy Environ. Sci.* **2012**, *5*, 6012−6021.
(9) Khnayzer, R. S.; McCusker, C. E.; Olaiya, B. S.; Castellano, F. N. *J. Am. Chem. Soc.* **2013**, *135*, 14068−14070.
(10) Luo, S.-P.; Mejía, E.; Friedrich, A.; Pazidis, A.; Junge, H.; Surkus, A.-E.; Jackstell, R.; Denurra, S.; Gladiali, S.; Lochbrunner, S.; Beller, M. *Angew. Chem., Int. Ed.* **2013**, *52*, 419−423.
(11) Karnahl, M.; Mejía, E.; Rockstroh, N.; Tschierlei, S.; Luo, S.-P.; Grabow, K.; Kruth, A.; Brüser, V.; Junge, H.; Lochbrunner, S.; Beller, M. *ChemCatChem.* **2014**, *6*, 82−86.
(12) Mejía, E.; Luo, S.-P.; Karnahl, M.; Friedrich, A.; Tschierlei, S.; Surkus, A.-E.; Junge, H.; Gladiali, S.; Lochbrunner, S.; Beller, M. *Chem.—Eur. J.* **2013**, *19*, 15972−15978.
(13) Neubauer, A.; Grell, G.; Friedrich, A.; Bokarev, S. I.; Schwarzbach, P.; Gärtner, F.; Surkus, A.-E.; Junge, H.; Beller, M.; Kühn, O.; Lochbrunner, S. *J. Phys. Chem. Lett.* **2014**, *5*, 1355−1360.
(14) Armaroli, N. *Chem. Soc. Rev.* **2001**, *30*, 113−124.
(15) van den Bosch, B.; Chen, H.-C.; van der Vlugt, J. I.; Brouwer, A. M.; Reek, J. N. H. *ChemSusChem* **2013**, *6*, 790−793.
(16) Dunsch, L. *J. Solid State Electrochem.* **2011**, *15*, 1631−1646.
(17) Kaim, W.; Fiedler, J. *Chem. Soc. Rev.* **2009**, *38*, 3373−3382.
(18) Kaeser, A.; Mohankumar, M.; Mohanraj, J.; Monti, F.; Holler, M.; Cid, J.-J.; Moudam, O.; Nierengarten, I.; Karmazin-Brelot, L.; Duhayon, C.; Delavaux-Nicot, B.; Armaroli, N.; Nierengarten, J.-F. *Inorg. Chem.* **2013**, *52*, 12140−12151.
(19) Penfold, T. J.; Karlsson, S.; Capano, G.; Lima, F. A.; Rittmann, J.; Reinhard, M.; Rittmann-Frank, M. H.; Braem, O.; Baranoff, E.; Abela, R.; Tavernelli, I.; Rothlisberger, U.; Milne, C. J.; Chergui, M. *J. Phys. Chem. A* **2013**, *117*, 4591−4601.
(20) McCusker, C. E.; Castellano, F. N. *Inorg. Chem.* **2013**, *52*, 8114−8120.
(21) Iwamura, M.; Watanabe, H.; Ishii, K.; Takeuchi, S.; Tahara, T. *J. Am. Chem. Soc.* **2011**, *133*, 7728−7736.
(22) Kaim, W.; Ernst, S. *J. Phys. Chem.* **1986**, *90*, 5010−5014.
(23) Bokarev, S. I.; Hollmann, D.; Pazidis, A.; Neubauer, A.; Radnik, J.; Kühn, O.; Lochbrunner, S.; Junge, H.; Beller, M.; Brückner, A. *Phys. Chem. Chem. Phys.* **2014**, *16*, 4789−4796.
(24) Hollmann, D.; Gärtner, F.; Ludwig, R.; Barsch, E.; Junge, H.; Blug, M.; Hoch, S.; Beller, M.; Brückner, A. *Angew. Chem., Int. Ed.* **2011**, *50*, 10246−10250.
(25) Tromp, M.; van Strijdonck, G. P. F.; van Berkel, S. S.; van den Hoogenband, A.; Feiters, M. C.; de Bruin, B.; Fiddy, S. G.; van der Eerden, A. M. J.; van Bokhoven, J. A.; van Leeuwen, P. W. N. M.; Koningsberger, D. C. *Organometallics* **2010**, *29*, 3085−3097.
(26) Streich, D.; Astuti, Y.; Orlandi, M.; Schwartz, L.; Lomoth, R.; Hammarström, L.; Ott, S. *Chem.—Eur. J.* **2010**, *16*, 60−63.
(27) Lomoth, R.; Häupl, T.; Johansson, O.; Hammarström, L. *Chem.—Eur. J.* **2002**, *8*, 102−110.
(28) Deb, B.; Dutta, D. K. *Polyhedron* **2009**, *28*, 2258−2262.
(29) Gärtner, F.; Boddien, A.; Barsch, E.; Fumino, K.; Losse, S.; Junge, H.; Hollmann, D.; Brückner, A.; Ludwig, R.; Beller, M. *Chem.—Eur. J.* **2011**, *17*, 6425−6436.
(30) Ellis, J. E.; Chen, Y. S. *Organometallics* **1989**, *8*, 1350−1361.
(31) Walther, B.; Hartung, H.; Böttcher, H.-C.; Baumeister, U.; Böhland, U.; Reinhold, J.; Sieler, J.; Ladriere, J.; Schiebel, H.-M. *Polyhedron* **1991**, *10*, 2423−2435.
(32) Cheah, M. H.; Borg, S. J.; Bondin, M. I.; Best, S. P. *Inorg. Chem.* **2004**, *43*, 5635−5644.
(33) Gimbert-Suriñach, C.; Bhadbhade, M.; Colbran, S. B. *Organometallics* **2012**, *31*, 3480−3491.
(34) Cheah, M. H.; Borg, S. J.; Best, S. P. *Inorg. Chem.* **2007**, *46*, 1741−1750.

(35) Tschierlei, S.; Ott, S.; Lomoth, R. *Energy Environ. Sci.* **2011**, *4*, 2340−2352.
(36) Tard, C.; Pickett, C. J. *Chem. Rev.* **2009**, *109*, 2245−2274.
(37) Garrou, P. E. *Chem. Rev.* **1985**, *85*, 171−185.
(38) Almeida Lenero, K. Q.; Guari, Y.; Kamer, P. C. J.; van Leeuwen, P. W. N. M.; Donnadieu, B.; Sabo-Etienne, S.; Chaudret, B.; Lutz, M.; Spek, A. L. *Dalton Trans.* **2013**, *42*, 6495−6512.
(39) Bradford, C. W.; Nyholm, R. S. *J. Chem. Soc., Dalton Trans.* **1973**, 529−533.